Article

Development of a Whole-Cell System Based on Genetically Modified Protoplasts to Detect Nickel Ions in Food Matrices

Monica De Caroli , Carla Perrotta , Patrizia Rampino *

Posted Date: 13 May 2024

doi: 10.20944/preprints202405.0859.v1

Keywords: whole-cell system; *Nicotiana tabacum* protoplasts; HSP promoter; heavy metals; food safety

 doi:10.20944/preprints202405.0859.v1

Article

Development of a Whole-Cell System Based on Genetically Modified Protoplasts to Detect Nickel Ions in Food Matrices

Monica De Caroli [1,2], Carla Perrotta [1] and Patrizia Rampino [1,*]

[1] Department of Biological and Environmental Sciences and Technologies, University of Salento, Via Monteroni 165, 73100, Lecce, Italy
[2] NBCF National Biodiversity Future Center, 90133 Palermo, Italy
* Correspondence: patrizia.rampino@unisalento.it

Abstract: Heavy metals are dangerous contaminants constituting a threat to human health because they persist in soils and are easily transferred into the food chain, causing damages to human health. Among heavy metals, nickel appears to be one of the most dangerous responsible for different disorders. Public health protection requires nickel detection in environment and food chains; a simple, rapid and sensitive method to detect nickel contamination is represented by biosensors. In this paper we report the setup of a whole-cell based system, in which protoplasts, obtained from *Nicotiana tabacum* leaves, were used as transducers to detect the presence of heavy metal ions and, in particular, nickel ions. Protoplasts were genetically modified with a plasmid containing the *GFP* reporter gene under the promoter region of a sunflower small *HSP* gene control. By this device the presence of heavy metal ions was detected. Thus, the possibility to use this whole-cell system as a novel tool to detect the presence of nickel ions in food matrices was assessed.

Keywords: whole-cell system; *Nicotiana tabacum* protoplasts; *HSP* promoter; heavy metals; food safety

1. Introduction

Heavy metals are considered the most dangerous contaminants for environment; they constitute a threat to human health, even when present in traces. The principal sources of heavy metal are industrial effluents discharge and fertilizers, responsible for soil contamination. The main threat for human health derives from the capability of metal ions to persist in soils, where they tend to accumulate and are easily transferred into the food chain [1,2] causing damages to human health. These contaminants raise a serious global issue, concerning the effect of heavy metals on food contamination and food safety [3,4]. Although it has been assessed that some heavy metals in trace amounts are nutritionally essential for healthy life, they can become toxic when accumulate in human soft tissues because are not metabolized. This causes a decrease in energy levels in vital organs, blood composition, and reduces mental and central nervous function [5].

Among heavy metals, nickel appears to be one of the most dangerous because it is naturally present in drink water as well as in many food matrices exposing population to its ingestion. Sensitivity to nickel prevalence varies in different countries in a range between 4-13.1% [6–8]. Nickel is extremely harmful for health because can cause different disorders such as kidney, lung and cardiovascular diseases, dermatitis and, sometimes, even some kind of cancer [9]. Therefore, public health protection certainly requires nickel detection in environment and food chains. At the present, the existing techniques used for trace analysis of heavy metals include chromatographic, voltammetric and spectroscopic methods. However, all these methods cannot be used for *in situ* analysis and are quite expensive. On the contrary, new tools such as biosensors can be used as a simple, rapid, and sensitive method to detect heavy metal contaminants, also by *in situ* analysis.

 doi:10.20944/preprints202405.0859.v1

Classical biosensors are analytical devices characterized by three elements: a biological recognition element, associated to a physical-chemical transducer, converting the biological response into a detectable signal, and a micro-electronic component able to amplify and convert the signal into a numeric record [10]. In particular, when a prokaryotic or eukaryotic cell represents a reporter system incorporating both biological recognition and transducer elements, the device is called "whole-cell biosensor" or, in other words, it constitutes a whole-cell detection system [5,11,12]. This kind of biosensor responds to the presence of contaminants or to physiological stresses producing a detectable cellular output signal. Generally, the cells used as biosensors are engineered to acquire the ability to behave as transducers or to amplify their sensitivity by introducing reporter genes controlled by promoters responding to environmental stimuli. Most of the cells type considered particularly useful for metal ions detection are genetically modified bacteria, although also eukaryotic cells, such as yeast, algae or protozoan can be used [5].

In this paper we report the setup of a whole-cell based system, in which protoplasts obtained from *Nicotiana tabacum* leaves were used as transducers, to detect the presence of heavy metal ions. The whole-cell detection system is based on the ability of plant cells to respond to environmental abiotic stresses such as the presence of metal ions, eliciting a molecular response. *N. tabacum* protoplasts were genetically modified with a plasmid containing the *GFP* reporter gene under control of the promoter region of a sunflower gene coding a small heat shock protein (HSP). This device was used to test the presence of nickel ions in different food matrices known to possess an high nickel content, exploring the possibility to use this biosensor as a novel tool to detect the presence of nickel ions in food matrices.

2. Results

2.1. Protoplasts Transformation and Immobilization

Protoplasts obtained from leaves of *N. tabacum* were transformed with p*35SGFP* or pPr*HSP17.6aGFP* plasmids, containing *GFP* gene under control of the constitutive *CAMV35S* or the inducible sunflower *HSP17.6a* promoters respectively, as described in Materials and Methods section. Afterwards, accurately prepared protoplasts were in part maintained in liquid K3 medium and in part immobilized in K3 medium containing agarose (0.6%) into 96 multi-well plates. Untransformed (WT) and transformed protoplasts, maintained in liquid K3 medium or immobilized in agarose, were tested for their viability by using fluorescein diacetate (FDA) assay. FDA is a fluorophore able to penetrate living and dead cells, but making fluorescent only the viable cells; in fact, the fluorescent labelling is due to fluorescein cleavage by cellular esterases, which are active only in viable cells [13], promoting the emission of green fluorescence [14]. Transformed and untransformed protoplasts, either in liquid K3 medium (floating) or immobilized in 0.6% agarose, were observed by confocal microscope. The results obtained, reported in Figure 1, indicate that immobilization does not alter the structure and viability of the transformed and untransformed protoplasts, as deduced by the spherical form of fluorescent cells.

 doi:10.20944/preprints202405.0859.v1

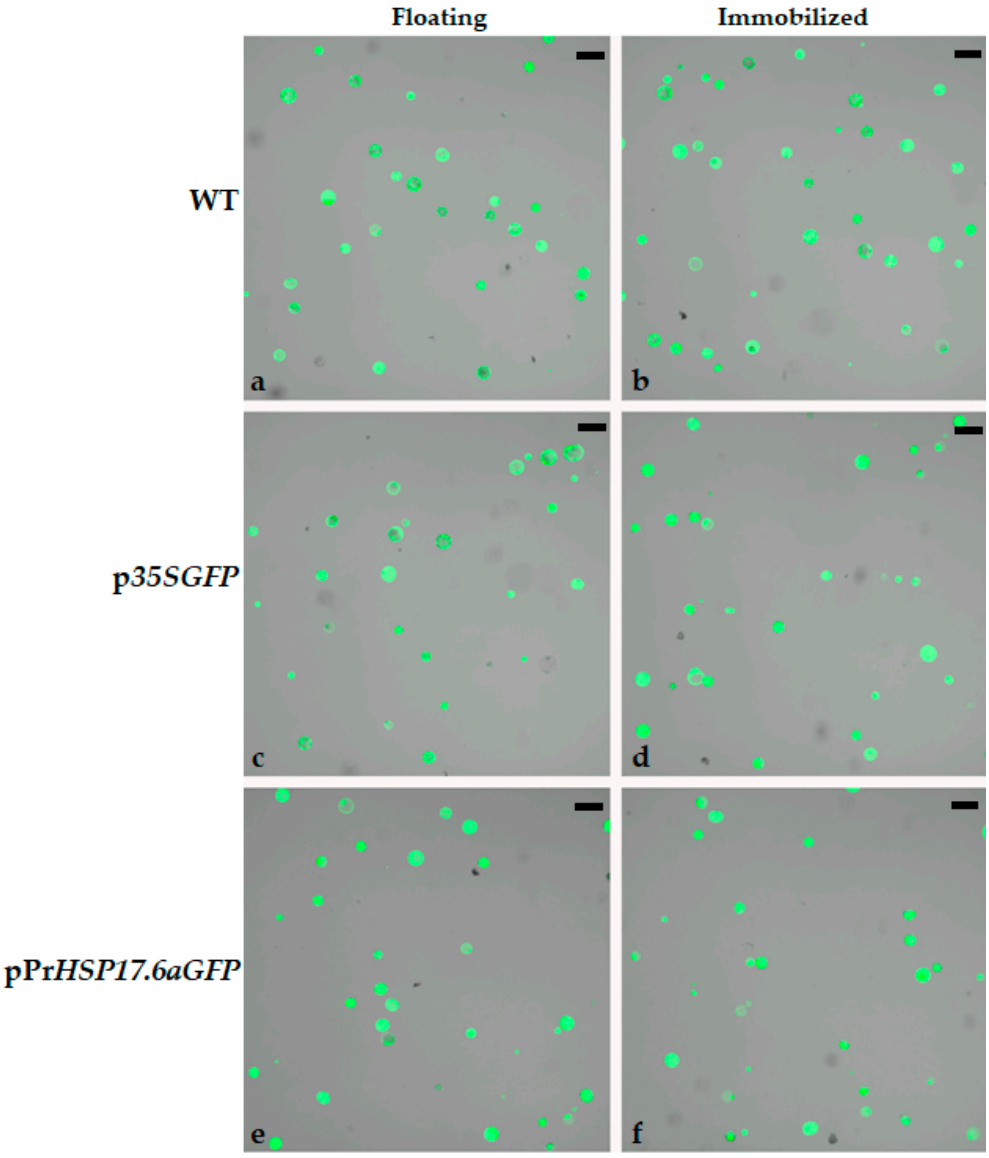

Figure 1. Confocal microscope images of tobacco protoplasts after FDA staining. **WT** untransformed protoplasts; **p*35SGFP*** Protoplast transformed with p*35SGFP* plasmid; **pPr*HSP17.6aGFP*** Protoplast transformed with pPr*HSP17.6aGFP* plasmid. **(a)**, **(c)** and **(e)** Floating protoplasts; **(b)**, **(d)** and **(f)** Protoplasts immobilized in K3 medium containing 0.6% agarose. Scale bars: 50 µm. Objective: 10x; zoom: 0.6.

Furthermore, the number of viable protoplasts was determined by FDA assay; the results are reported in Table 1 and indicate that the percentage of viable protoplasts is almost the same for untransformed and transformed protoplasts, as well as for floating protoplasts (maintained in K3 medium) and those immobilized in K3 medium containing 0.6% agarose.

 doi:10.20944/preprints202405.0859.v1

Table 1. Protoplast viability (%) of untransformed and p*35SGFP* or p*PrHSP17.6aGFP* transformed protoplasts floating in K3 medium or immobilized in K3 medium containing 0.6% agarose.

	Floating protoplasts (%)	Immobilized protoplast (%)
WT	98.77 ± 1.23	97.70 ± 2.30
p*35SGFP*	99.05 ± 0.95	98.44 ± 1.56 [1]
pPr*HSP17.6aGFP*	97.87 ± 2.13	98.65 ± 1.35

Each value represents the mean of three independent measurements ± SE. WT, untrasformed protoplasts; p*35SGFP*, protoplasts transformed with p*35SGFP* plasmid; pPr*HSP17.6aGFP*, protoplasts transformed with pPr*HSP17.6aGFP* plasmid.

Immobilized protoplasts were analyzed for auto-fluorescence emission. Fluorescence was measured in wild type as well as in engineered protoplasts, after 2, 3, 4, 7 hours from immobilization. A fluorescent signal was detected for all the protoplast samples. As reported in Figure 2, the level of the signal is almost the same during time (after 2 to 7 h) for each group of protoplasts. Moreover, as expected, the fluorescence signal detected for p*35SGFP* transformed protoplasts is always higher than the fluorescence signal detected for untransformed protoplasts (WT), as well as for p*PrHSP17.6aGFP* transformed protoplasts. Statistical analysis indicated that there is no statistically significant difference in fluorescence signal values, measured at the various time points, within each protoplasts group (WT, p*35SGFP* and pPr*HSP17.6aGFP* transformed protoplasts); moreover, no significant difference was observed between the WT and pPr*HSP17.6aGFP* transformed protoplast groups. On the contrary, a highly significant difference ($p<0.001$) was observed between the p*35SGFP* transformed protoplasts group and the WT group or the pPr*HSP17.6aGFP* transformed protoplasts group (Figure 2).

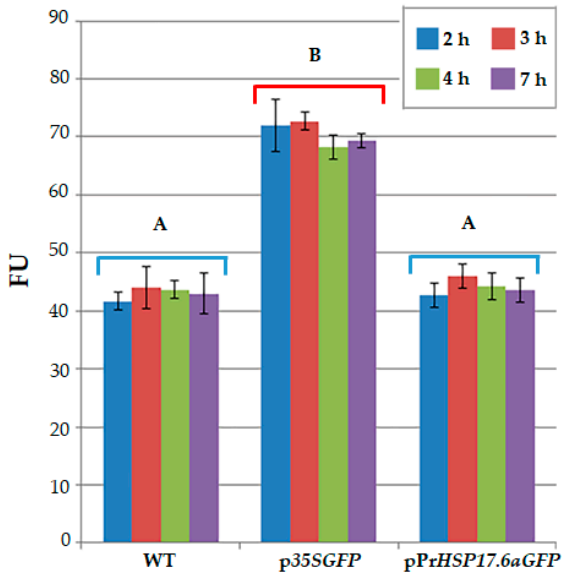

Figure 2. Evaluation of fluorescence by fluorometer after 2, 3, 4, 7 hours from immobilization of untransformed protoplasts (**WT**), protoplasts transformed with p*35SGFP* plasmid (**p*35SGFP***), and protoplasts transformed with p*PrHSP17.6aGFP* plasmid (**p*PrHSP17.6aGFP***). Each value represents the mean of three independent measurements ± SD. Different uppercase letters indicate significant differences among the FU values ($p<0.001$).

To verify that differences in fluorescence were due to *GFP* gene expression driven by *CAM35S* constitutive promoter, protoplasts were observed by confocal microscope. The data obtained indicate that differences in fluorescence, detected by the fluorometer, are due to the expression of GFP, since only p*35SGFP* transformed protoplasts exhibited a green fluorescent signal when observed by the confocal microscope (Figure 3).

 doi:10.20944/preprints202405.0859.v1

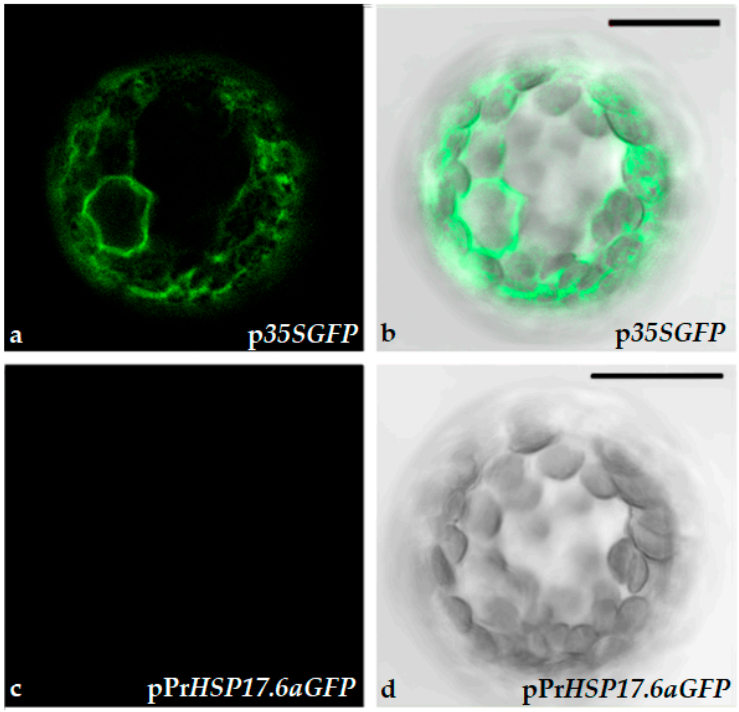

Figure 3. Confocal microscope images of immobilized tobacco protoplasts. **(a)** and **(b)** Protoplasts transformed with p*35SGFP* plasmid; **(c)** and **(d)** Protoplasts transformed with p*PrHSP17.6aGFP* plasmid. **(b)** and (**d)** Bright field. Scale bars: 20 μm. Objective 40x, zoom 2.0.

2.2. Responsiveness of Engineered Protoplast to Heavy Metal Ions

To test the ability of engineered protoplasts to sense metal ions presence, immobilized protoplasts were added with 50 μL of 20 μM each $AlCl_3$, $CdSO_4$, $CoCl_2$, $CuSO_4$, $NiCl_2$, $ZnSO_4$ at room temperature, fluorescence was measured by fluorometer after 1, 2, 3, and 4 h. The values of fluorescence were measured in protoplasts transformed with p*35SGFP* plasmid, used as control, as well as in protoplasts transformed with p*PrHSP17.6aGFP* plasmid. Values detected are shown in Figure 3 and indicate that the signals of p*35SGFP* transformed protoplasts remain unchanged during time course with all salt treatments. Fluorescence signals of p*PrHSP17.6aGFP* transformed protoplasts increased during time course, reaching the maximum level after 2 h and remaining almost the same afterwards. Only when $CuSO_4$ was used, the maximum induction was reached after 3 h and the fluorescence signal declined thereafter (Figure 4).

 doi:10.20944/preprints202405.0859.v1

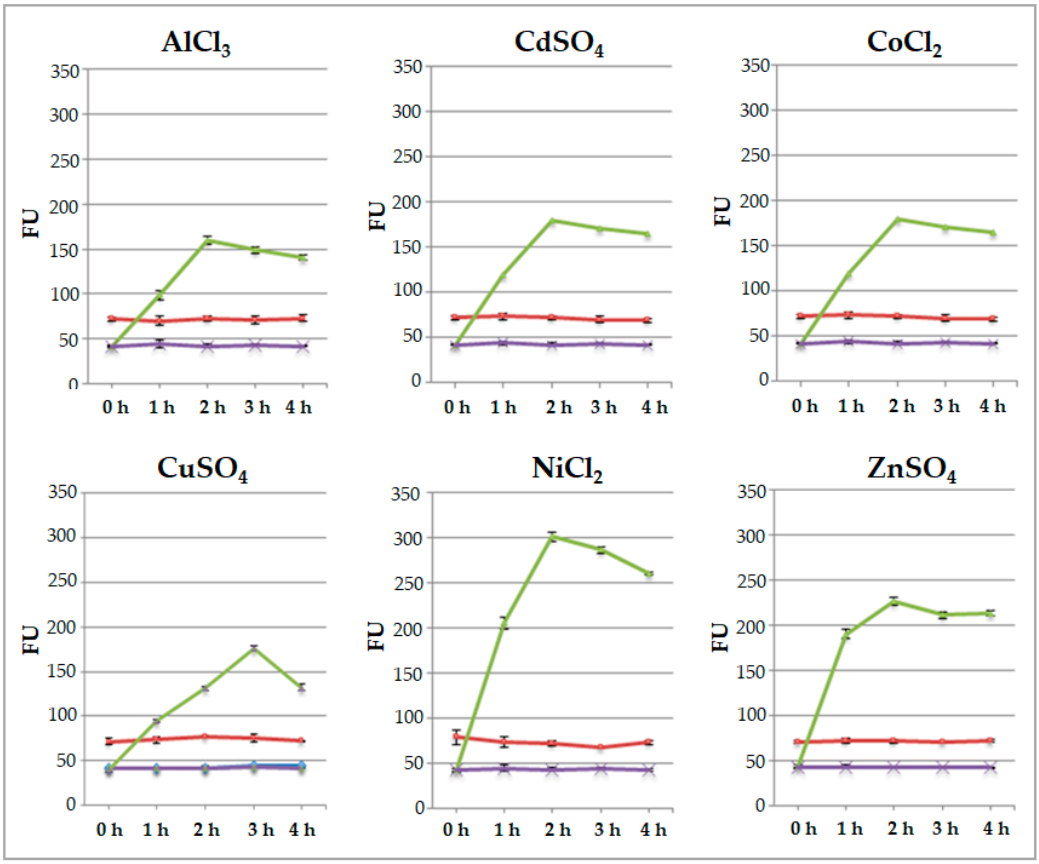

Figure 4. Evaluation of fluorescence by fluorometer after 1, 2, 3 and 4 hours from protoplasts immobilization. **Red line**: protoplasts transformed with p*35SGFP* plasmid; **violet line**: untreated protoplasts transformed with p*PrHSP17.6aGFP* plasmid; **green line**: protoplasts transformed with p*PrHSP17.6aGFP* plasmid plus metal ion solutions. Each value represents the mean of three independent measurements ± SD.

Moreover, the data obtained indicate that the signal intensity depends on the specific metal ion added. In particular, after 2 hours, in the case of $NiCl_2$ treatment the signal is more of 7-fold higher than the untreated protoplasts, more or less 5.5-fold higher after treatment with $ZnSO_4$ and $CoCl_2$, 4.5-fold higher using $AlCl_3$ and $CdSO_4$ salts; following $CuSO_4$ treatment the maximum value was 4-fold higher (Figure 5).

Comparison among the relative fluorescence values reached by engineered protoplasts indicates that these values are similar when engineered protoplasts were treated with $AlCl_3$ and $CdSO_4$ or with $CuSO_4$, in fact, in these cases no statistically significant difference was observed in relative fluorescence values. The fluorescence signals were almost the same also in the presence of $CoCl_2$ and $ZnSO_4$ and no statistically significant difference was observed also in this case. On the contrary, statistically significant differences were observed when florescence signal values relative to protoplasts treated with Ni ions were compared with all the other value groups. In particular, highly significant differences ($p<0.001$) were observed when values reached by protoplasts treated with Ni ions were compared to the ones obtained after treatment with Al, Cd and Cu ions, while significant differences ($p<0.05$) were observed when they were compared to the ones obtained after treatment with Co and Zn ions (Figure 5).

Preprints.org (www.preprints.org) | NOT PEER-REVIEWED | Posted: 13 May 2024 doi:10.20944/preprints202405.0859.v1

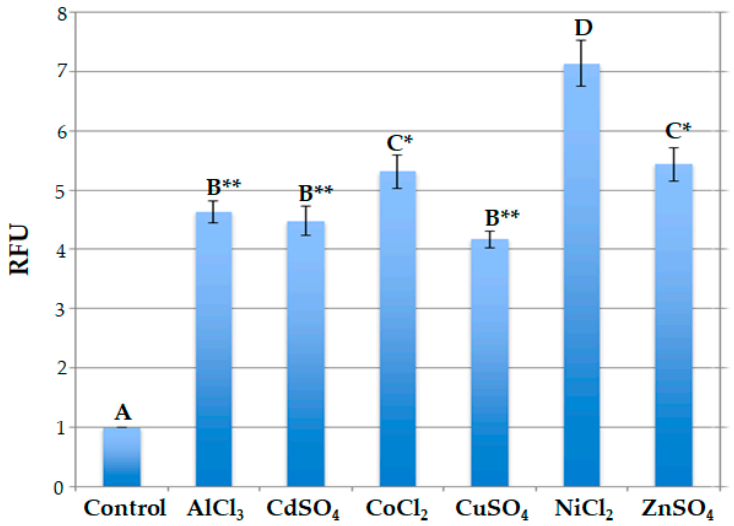

Figure 5. Relative fluorescence (expressed as Relative Fluorescence Units, RFU) at the maximum level of detection of protoplasts transformed with p*PrHSP17.6aGFP* and treated with different metal ions. Each value represents the mean of three independent measurements ± SD. Uppercase letters indicate statistically different values among the various protoplast groups. Asterisks correspond to statistically different values between the $NiCl_2$ treated protoplasts and each other different group (*, significant difference, $p < 0.05$; **, highly significant difference, $p<0.001$).

These data were confirmed by confocal observations and fluorescence quantification of protoplasts treated with the six different heavy metal ions (Figure 6). Protoplasts tested with all heavy metal ion treatments appeared fluorescent, although with different intensity and fluorescence patterns. The compartments of the secretion pathway (nuclear membrane in continuity with the endoplasmic reticulum and the Golgi complex) were clearly evident in protoplasts characterized by a higher level of GFP expression, i.e. protoplast treated with $CoCl_2$, $NiCl_2$ and $ZnSO_4$,

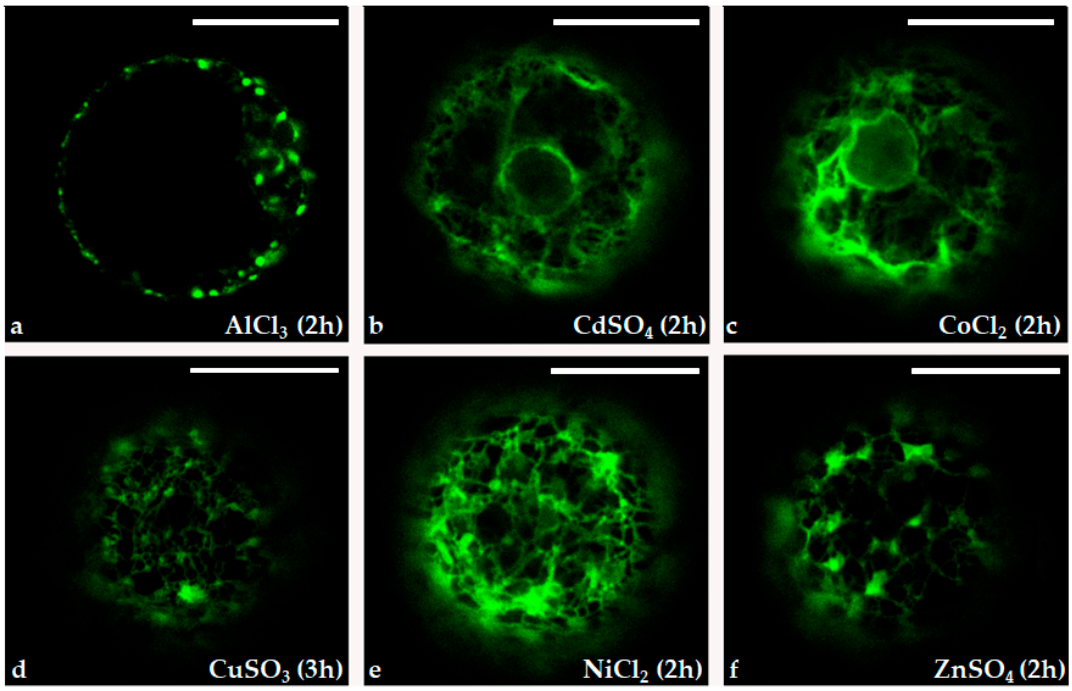

Figure 6. Confocal microscope images of the immobilized protoplasts transformed with p*PrHSP17.6aGFP* plasmid in presence of 20 µM $AlCl_3$ **(a),** $CdSO_4$ **(b)**, $CoCl_2$ **(c)**, $CuSO_4$ **(d)**, $NiCl_2$ **(e)** and $ZnSO_4$ **(f)**. Scale bars: 20 µm. Objective: 40x; zoom: 2.0.

Preprints.org (www.preprints.org) | NOT PEER-REVIEWED | Posted: 13 May 2024 doi:10.20944/preprints202405.0859.v1

These data were confirmed also by fluorescence index values (Table 2) Comparison of the fluorescence index value obtained after $NiCl_2$ treatment indicates significant differences in respect to all other salt treatments.

Table 2. Fluorescence index given by the mean of GFP pixels intensity per protoplast transformed with p*PrHSP17.6aGFP* and treated with the different metal ions. Differences between $NiCl_2$ treated protoplasts and each different metal ion were significant (*, $p < 0.05$,) or highly significant (**, $p<0.001$).

	Mean±SD of GFP pixel intensity per protoplast
$AlCl_3$ (2 h)	4.76±0.43**
$CdSO_4$ (2 h(	4.21±0.46**
CoCl2 (2 h)	5.27±0.66**
$CuSO_4$ (3 h)	4.02±0.51**
NiCl2 (2 h)	7.30±0.46
$ZnSO_4$ (2 h)	5.18±0.52*

Since all the data indicated that nickel ions are the best inducers of fluorescence, to better characterize the response of the engineered protoplasts to this type of treatment, they were subjected for 2 hours to various nickel ion concentrations, from 2 µM to 40 µM. Results obtained indicate that, rising Ni ion concentrations, the signal increases reaching the maximum value at the concentration of 20 µM $NiCl_2$; thereafter the signal reached the plateau using higher Ni ion concentrations (Figure 7).

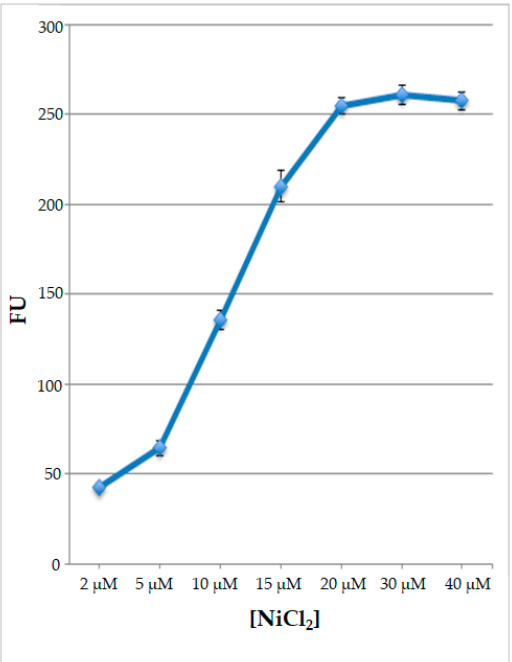

Figure 7. Values of fluorescence, expressed as Fluorescence Units (FU) of protoplasts transformed with p*PrHSP17.6aGFP* plasmid and treated with different $NiCl_2$ concentrations. Each value represents the mean of three independent measurements ± SD.

2.3. Nickel Ions Detection in Different Food Matrices

Considering that nickel ions appear the most efficient in eliciting fluorescence signal and that they are naturally present in many food matrices, the ability of the whole-cell system to detect Ni ions in food was tested. For this, the pPrHSP17.6aGFP engineered protoplasts were challenged against various food matrices, known to be “high nickel foods” (canned peeled tomatoes, cocoa powder, grounded tea leaves, oat flour) or “low nickel foods”, namely bread wheat flour type 00, the most

 doi:10.20944/preprints202405.0859.v1

refined bread wheat flour [15–17]. All the food matrices were tested after adding exogenous nickel ions. $NiCl_2$ solution was added to reach a final concentration of 20 µM. The results, reported in Figure 8, indicate that the level of fluorescence signal is higher than that measured after treatment with nickel ions only, depending on the matrix utilized. The highest signal was obtained with grounded tea leaves (FU 538) while the lowest signal was obtained with bread wheat flour type 00 (FU 310).

Subsequently, protoplasts were challenged against the different food matrices only. In general all food matrices are able to induce an increase in GFP expression. Results obtained, reported in Figure 8, confirm that grounded tea leaves are the most effective inducers (FU 270), while bread wheat flour (type 00) is the least effective inducer (FU 85). In particular, for grounded tea leaves the level of induction was 6-fold higher than that obtained in untreated protoplasts, for cocoa powder it was 5-fold, for canned peeled tomatoes it was 4-fold, for oat flour it was 3-fold, and for type 00 wheat flour it was only 2-fold with respect to the same control, represented by untreated transformed protoplasts.

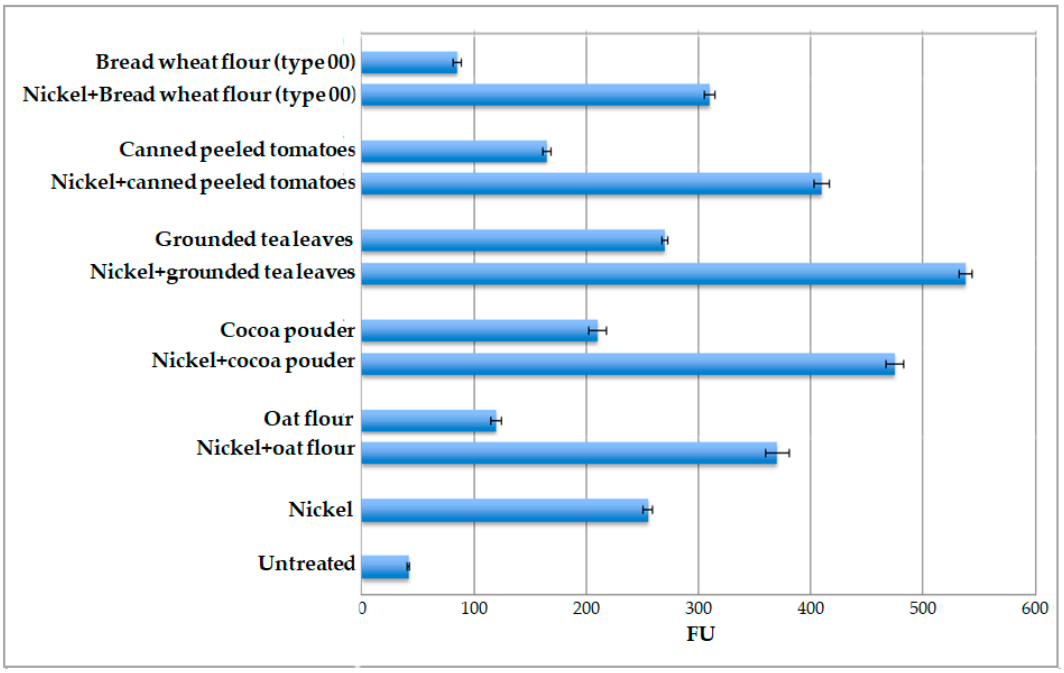

Figure 8. Values of fluorescence, expressed in Fluorescence Units (FU) of protoplasts transformed with p*PrHSP17.6aGFP* plasmid plus the addition of different food matrices (in the presence or absence of 20 µM nickel ions) for 2 h. Protoplasts transformed with p*PrHSP17.6aGFP* plasmid added only with nickel ions (**Nickel**) and untreated protoplasts (**Untreated**) were used as controls. Each value represents the mean of three independent measurements ± SD.

3. Discussion

Technological processes and agrochemical treatments are the main responsible for the contamination of food products and for the reduction of food nutritional value. The development of safe and accurate analytical methodologies for water and food control is crucial for detection, analysis and diagnosis of a wide range of compounds affecting food quality and healthiness. Among the worst contaminants there are heavy metal ions dangerous, because they are widely present in the environment and also because they are easily transferred from soil and water to living organisms [3,18].

Plants exposed to adverse environmental conditions (biotic or abiotic stresses) have developed complex molecular mechanisms to protect cell homeostasis and minimize the potential damages caused by these stimuli [19]. In general, plant stress response is based on activation and/or inactivation of gene expression rapidly triggered after perception of the stress. The rapidity of the response is due to the presence of different stress-responsive *cis* elements in the promoter region of

 doi:10.20944/preprints202405.0859.v1

these genes [20]. The most important group of genes participating to stress response is constituted by the *heat shock* gene family. These genes are activated not only by heat stress but also by other stressful environmental conditions, such as the presence of heavy metal ions [21,22].

With the aim to test the ability of the promoter region of a plant small *HSP* gene to sense the presence of heavy metal ions in different food matrices, *N. tabacum* protoplasts were transformed with a plasmid containing the *GFP* gene controlled by the promoter region of the sunflower *HaHSP17.6a* gene. This specific promoter was chosen on the basis of the characterization, in a previous work, of the *HaHSP17.6a* gene reported to be inducible, in sunflower seedlings, by heat stress as well as by other stimuli and in particular by the presence of heavy metal ions [22].

The data obtained *in vitro* using this transient expression system assessed that the promoter region of *HaHSP17.6a* gene is activated by all the metal ions tested, although at different level, confirming its inducibility, already demonstrated *in vivo* in sunflower seedlings [22]; the data also indicated that *HaHSP17.6a* promoter exhibits the best sensitivity to Ni ions.

Having assessed promoter inducibility, the engineered protoplast system was tested also for its ability to sense the presence of heavy metal ions, with particular regard to Ni, in different food matrices. Considering that systemic nickel allergy syndrome affects a large part of population, the creation of a more sensitive and effective tool for the rapid and *in situ* detection of high concentration of Ni ions in food could play an important role for future improvements in food analysis. Food matrices utilized in this work were chosen mostly on the basis of their already known nickel content, according to their classification or as "high Ni foods" or as "low Ni foods" [15,17,23–25].

The first step of this part of the work was aimed at verifying whether the molecular composition of food matrices can "quench" nickel ions present in a solution. In order to do that, determination of fluorescence emission was performed adding to the different matrices a known quantity of $NiCl_2$. Subsequently, the same tests were repeated using food matrix alone. In both cases induction of fluorescence was detectable, and it specifically varied according to the food matrix assayed indicating that none of the food matrices utilized have a molecular structure able to interfere with the biological detection of nickel ions present in the test solution.

In conclusion, all together the data obtained indicate that the engineered immobilized protoplasts system set up is a useful tool to detect the presence of nickel ions in food. To our knowledge this is so far the first example of biosensor to detect traces of heavy metal ions in food, based on genetically engineered plant protoplasts. Starting from these data, a wider use of the biosensor realized, aimed at the detection of other heavy metal ions in different matrices can be hypothesized also considering that whole-cell biosensors appear the most suitable detection tool, not only because they are chip and portable but also because they are specifically designed to have high sensitivity in detecting heavy metal ions in trace levels. In other words, whole-cell biosensors can be considered the best way to measure heavy metal ions in food, thus contributing to reach larger benefits to consumers health in relationship to food production and safety.

4. Materials and Methods

4.1. Plasmids Construction

A DNA fragment, corresponding to the promoter region of sunflower small *HSP17.6a* gene [22], was amplified using the primers For-tgcctcgaggtagtacacggtg and Rev-gtaaaattgttcaacgtgttctagaggat; primers contained restriction sites, to generate *Xho*I and *Bam*HI ends. PCR was performed on genomic DNA obtained from sunflower seedlings (*Heliantus annuus* L., cv. Gloriasol) using "Pure Link Plant Total DNA purification" kit (Invitrogen, Carlsbad, CA, USA), according to supplier's instruction. In order to verify amplicons identity, the PCR product were purified and sequenced using standard procedures; the DNA sequence, 1769 bp long, was compared with the corresponding genomic clone (accession number AJ306557.2). The DNA fragment obtained was cloned into a vector containing the *GFP* (Green Fluorescent Protein) gene followed by *nopaline synthase* gene (*Nos*) terminator, previously digested with *Xho*I and *Bam*HI; the plasmid obtained was named pPr*HSP17.6aGFP*. A plasmid containing the *GFP* gene under control of *CAMV35S* promoter, named p*35SGFP*, was used as control.

 doi:10.20944/preprints202405.0859.v1

4.2. Protoplasts Preparation, Transformation and Immobilization

N. tabacum cultivar SR1 protoplasts were prepared from leaves of 7-8 weeks old plants. Transformation was performed as previously described by Gullì and coworkers [26] using PEG-mediated direct gene transfer. Ten micrograms of each constructed plasmid were used for the transformation of ~ 600,000 protoplasts. Protoplast suspension was gently mixed with a solution of 0.6% agarose in K3 medium [27] at 40°C; 150 µl of the mixture were distributed in a multiwall plate and solidification was completed after 30 min at room temperature. Immobilized protoplasts were kept at room temperature until stress treatments were performed.

4.3. Protoplasts Stress Treatments with Different Heavy Metal Ions

Transformed protoplasts were subjected to metal ion stress by adding 50 µL of 20 µM each $AlCl_3$, $CdSO_4$, $CoCl_2$, $ZnSO_4$, or 2 µM, 5 µM, 10 µM, 15 µM, 20 µM, 30 µM and 40 µM $NiCl_2$, at room temperature and observed after 1, 2, 3 and 4 h for fluorescence determination. Controls were: wild type protoplasts (WT) and protoplasts transformed with the p*35SGFP* plasmid, subjected to stress, as well as WT protoplasts, protoplasts transformed with the p*35SGFP* plasmid and pPr*HSP17.6aGFP* not subjected to stress.

4.5. FDA Assay for Protoplast Viability Estimation

Fluorescein diacetate (FDA) staining was used to determine the viability of protoplasts. Fifty µL of the K3 medium containing untransformed or transformed protoplasts were transferred into a microtube; 1 µL of 0.2% FDA solution, dissolved in acetone, was added and incubated at room temperature for 2 min. All FDA treated protoplasts were observed in K3 culture medium and after agarose (0.6%) immobilization. Only viable protoplasts appeared green fluorescent at the confocal laser microscope (LSM 710, Carl Zeiss, Oberkochen, Germany). For the viability measurements, three images for each sample were selected; the percentage of protoplast viability was expressed as the ratio between the number of the fluorescent protoplasts and the total number of protoplasts ×100. Each experiment was repeated three times.

4.6. Confocal Microscopy and Fluorescence Determination

For protoplasts observation, a laser scanning confocal microscope (LSM 710, Zeiss) was used. To control protoplasts viability after transformation and/or immobilization, protoplasts were observed in their culture medium and after agarose immobilization. To detect GFP or FDA fluorescence, a 488 nm argon ion laser line was used, and the emission was recorded with 505–530 nm filter set; while chlorophyll epifluorescence was detected with the filter >650 nm and eliminated, after He-Ne laser excitation at 543 nm as previously reported [28]. The power of each laser line, the gain, and the offset were identical for each experiment so that the images were comparable. For fluorescence quantification, the Profile Tool of the ZEN2012 program of the LSM 710 confocal microscope was used. The mean of pixel intensities relative to GFP channel was used for fluorescence quantification; 20 protoplasts for each treatment were measured to produce the quantification analysis and three independent experiments were performed. Images were processed using Adobe Photoshop 7.0 software (Mountain View, CA, United States). Protoplasts fluorescence was also measured using Infinite F200 fluorometer (TECAN, Männedorf, Switzerland) set as follows: excitation 485 nm (±20) and emission 510-560 nm. Fluorescence values are presented as arbitrary fluorescence units (FU) or as relative fluorescence unit (RFU), namely the ratio of the fluorescence of the treated sample to that of the untreated control (response ratio). All data are the mean of three different measurements.

4.7. Food Matrices Utilized for Nickel Ions Detection

Food matrices utilized to assess the responsiveness of engineered protoplasts to metal ions presence in food were: oat flour, cocoa powder, grounded tea leaves, canned peeled tomatoes, bread wheat flour (type 00). Two grams of each food matrix were added to 8 mL of sterile distilled water

 doi:10.20944/preprints202405.0859.v1

and stirred for 2 h. One mL was centrifuged at 13000 rpm for 2 min, 50 µL of supernatant were added to immobilized protoplasts.

4.8. Statistical Analysis

Statistical analysis was performed using the SigmaStat version 3.11 software (Systat Software Inc., Chicago, IL) as appropriate. The viability of protoplasts floating in K3 buffer or immobilized in 0.6% agarose were compared using Student's t-test The protoplast fluorescence values, measured fluorometrically or by confocal microscope tools, were analysed using appropriate statistical tests. All values were expressed as means ± standard deviation of at least three independent replicated experiments (n = 3). A p value ≤0.05 was considered statistically significant.

Author Contributions: Conceptualization, P.R. and C.P.; methodology, M.D.C. and P.R.; software, M.D.C.; validation, M.D.C, C.P. and P.R.; investigation, M.D.C. and P.R.; resources, P.R.; data curation, P.R.; writing—original draft preparation, M.D.C, C.P. and P.R.; writing—review and editing, C.P. and P.R.; supervision, P.R. All authors have read and agreed to the published version of the manuscript.

Acknowledgments: The authors wish to thank Prof. G. Dalessandro for critical reading of the manuscript.

Funding: This research received no external funding.

Institutional Review Board Statement: Not applicable.

Informed Consent Statement: Not applicable.

Data Availability Statement: The original contributions presented in this study are included in the article.

Conflicts of Interest: The authors declare no conflicts of interest.

References

1. Kabata-Pendias, A.; Mukherjee, A.B. Trace Elements from Soil to Human 2007. Springer-Verlag, Berlin, 23. https://doi.org/10.1007/978-3-540-32714-1.
2. Taghavi, M.; Darvishiyan, M.; Momeni,; M.; Eslami, H.; Fallahzadeh, R.A.; Zarei, A. Ecological risk assessment of trace elements (TEs) pollution and human health risk exposure in agricultural soils used for saffron cultivation. *Sci. Rep.* **2023**, *13*, 4556. https://doi.org/10.1038/s41598-023-31681-x.
3. Rai, P.K.; Lee, S.S.; Zhang, M.; Tsang, Y.F.; Kim, K.-H. Heavy metals in food crops: Health risks, fate, mechanisms, and management. *Environ. Int.* **2019**, *125*, 365–385. https://doi.org/10.1016/j.envint.2019.01.067.
4. Munir, N.; Jahangeer, M.; Bouyahya, A.; Omari, N.E.; Ghchime, R.; Balahbib, A.; Aboulaghras, S.; Mahmood, Z.; Akram, M.; Shah, S.M.A.; et al. Heavy Metal Contamination of Natural Foods Is a Serious Health Issue: A Review. *Sustainability* **2022**, *14*, 161. https://doi.org/10.3390/su14010161.
5. Gutiérrez, J.C.; Amaro, F.; Martin-Gonzáles, A. Heavy metal whole-cell biosensor using eukaryotic microorganism: An update critical review. *Front. Microbiol.* **2015**, *6*, 48. https://doi.org/10.3389/fmicb.2015.00048.
6. Lusi, E.A.; Di Ciommo, V.M.; Patrissi,T.; Guarascio, P High prevalence of nickel allergy in an overweight female population: A pilot observational analysis. *PLoS ONE* **2015**, *10*, e0123265. https://doi.org/10.1371/journal.pone.0123265.
7. Venter, C. Food Hypersensitivity: Diagnosing and Managing Food Allergies and Intolerances. *J. Allergy* **2012**, *2012*, 576017. https://doi.org/10.1155/2012/576017.
8. Anchidin-Norocel, L.; Savage, W.K.; Gutt, G.; Amariei, S. Development, Optimization, Characterization, and Application of Electrochemical Biosensors for Detecting Nickel Ions in Food. *Biosensors* **2021**, *11*, 519. https://doi.org/10.3390/bios11120519.
9. Genchi, G.; Carocci, A.; Lauria , G.; Sinicropi, M.S.; Catalano, A. Nickel: Human Health and Environmental Toxicology. Int. J. Environ. Res. Public Health **2020**, *17*, 679. https://doi.org/10.3390/ijerph17030679.
10. Belkin, S. Microbial whole-cell sensing systems of environmental pollutants. *Curr. Opin. Microbiol.* **2003**, *6*, 206–212. https://doi.org/10.1016/s1369-5274(03)00059-6.
11. Liu, C.; Yu, H.; Zhang, B.; Liu, S.; Liu, C.-g.; Li, F.; Song, H. Engineering whole-cell microbial biosensors: Design principles and applications in monitoring and treatment of heavy metals and organic pollutants. Biotechnol. Adv. **2022**, *60*, 108019. https://doi.org/10.1016/j.biotechadv.2022.108019.

12. Chen, S.; Chen, X.; Su, H.; Guo, M.; Liu, H. Advances in Synthetic-Biology-Based Whole-Cell Biosensors: Principles, Genetic Modules, and Applications in Food Safety. *Int. J. Mol. Sci.* **2023**, *24*, 7989. https://doi.org/10.3390/ijms24097989.
13. Schoor, S.; Lung, S.C.; Sigurdson, D.; Chuong, S.D. Fluorescent Staining of Living Plant Cells. In: Yeung, E.C.T.; Stasolla, C.; Sumner, M.J.; Huang, B.Q. (eds) Plant Microtechniques and Protocols. 2015 Springer Cham Heidelberg, New York, pp 153-165. https://doi.org/10.1007/978-3-319-19944-3.
14. Widholm, J.M. The use of fluorescein diacetate and phenosafranine for determining viability of cultured plant cells. Stain Technol. **1972**, *47*, 189–194. https://doi.org/ 10.3109/10520297209116483.
15. Borghini, R.; De Amicis, N.; Bella, A.; Greco, N.; Donato, G.; Picarelli, A. Beneficial Effects of a Low-Nickel Diet on Relapsing IBS-Like and Extraintestinal Symptoms of Celiac Patients during a Proper Gluten-Free Diet: Nickel Allergic Contact Mucositis in Suspected Non-Responsive Celiac Disease. *Nutrients* **2020**, *12*, 2277. https://doi.org/. https://doi.org/10.3390/nu12082277.
16. Cappelli, A.; Bini, A.; Cini, E. The Effects of Storage Time and Environmental Storage Conditions on Flour Quality, Dough Rheology, and Biscuit Characteristics: The Case Study of a Traditional Italian Biscuit (Biscotto di Prato). Foods **2022**, *11*, 209. https://doi.org/ 10.3390/foods11020209.
17. Greco, M.; Pisano, A.; Mezzatesta, L.; Pettinelli, M.; Meacci, A.; Pignataro, M.G.; Giordano, C.; Picarelli, A. New Insights and Evidence on "Food Intolerances": Non-Celiac Gluten Sensitivity and Nickel Allergic Contact Mucositis. *Nutrients* **2023**, *15*, 2553. https://doi.org/ 10.3390/nu15102353.
18. Scutarsu, E.C.; Trinca, L.C. Heavy Metals in Foods and Beverages: Global Situation, Health Risks and Reduction Methods. *Foods* **2023**, *12*, 3340. https://doi.org/ 10.3390/foods12183340.
19. Lamers, J.; van der Meer, T.; Testerink, C. How Plants Sense and Respond to Stressful Environments. *Plant Physiol.* **2022**, *182*, 1624–1635. https://doi.org/ 10.1104/pp.19.01464.
20. Wu, J.; Gao, T.; Hu, J.; Zhao, L.; Yu, C.; Ma, F. Research advances in function and regulation mechanisms of plant small heat shock proteins (sHSPs) under environmental stresses. *Sci. Total Environ.* **2022**, *825*, 154054. https://doi.org/ 10.1016/j.scitotenv.2022.154054.
21. Gullì, M.; Rampino, P.; Lupotto, E.; Marmiroli, N.; Perrotta, C. The effect of heat stress and cadmium ions on the expression of a small *hsp* gene in barley and maize. *J. Cer. Sci.* 2005, *42*, :25–31. https://doi.org/10.1016/j.jcs.2005.01.006.
22. Rampino, P.; Mita, G.; Assab, E.; De Pascali, M.; Giangrande, E.; Treglia, A.S.; Perrotta, C. Two sunflower *17.6HSP* genes, arranged in tandem and highly homologous, are induced differently by various elicitors. *Plant Biol.* **2010**, *12*, 13–22. https://doi.org/ 10.1111/j.1438-8677.2009.00200.x.
23. Picarelli, A.; Di Tola, M.; Vallecoccia, A.; Libanori, V.; Magrelli, M.; Carlesimo, M.; Rossi, A. Oral mucosa patch test: A new tool to recognize and study the adverse effects of dietary nickel exposure. *Biol. Trace Elem. Res.* **2011**, *139*, 151–159. https://doi.org/10.1007/s12011-010-8652-y.
24. Pizzutelli, S. Systemic nickel hypersensitivity and diet: Myth or reality? *Eur. Ann. Allergy Clin. Immunol.* **2011**, *43*, 5–18.
25. Rizzi, A.; Nucera, E.; Laterza, L.; Gaetani, E.; Valenza, V.; Corbo, G.M.; Inchingolo, R.; Buonomo, A.; Schiavino, D.; Gasbarrini, A. Irritable Bowel Syndrome and Nickel Allergy: What Is the Role of the Low Nickel Diet? *J. Neurogastroenterol. Motil.* **2019**, *23*, 101–108. https://doi.org/ 10.5056/jnm16027.
26. Gullì, M.; De Pascali, M.; Perrotta, C.; Rampino, P. A stress-related transcription factor belonging to the YL-1 family is differently regulated in durum wheat cultivars differing in drought sensitivity. *Plant Physiol. Biochem*. **2022**, *170*, 307–315. https://doi.org/ 10.1016/j.plaphy.2021.12.016.
27. Freydl, E.; Meins, F.Jr.; Boller, T.; Neuhaus, J.M. Kinetics of prolyl hydroxylation, intracellular transport and C-terminal processing of the tobacco vacuolar chitinase. Planta **1995**, *197*, 250–256.
28. De Caroli, M.; Lenucci, M.S.; Manualdi, F.; Dalessandro, G.; De Lorenzo, G.; Piro, G. Molecular dissection of *Phaseolus vulgaris* polygalacturonase-inhibiting protein 2 reveals the presence of hold/release domains affecting protein trafficking toward the cell wall. *Front. Plant Sci.* **2015**, *6*, 660. https://doi.org/ 10.3389/fpls.2015.00660.